Journal of Alloys and Compounds 654 (2016) 240–245

Contents lists available at ScienceDirect

Journal of Alloys and Compounds

journal homepage: http://www.elsevier.com/locate/jalcom

Letter

Influence of Sm^{3+} substitutions for Nd^{3+} on the microwave dielectric properties of $(Nd_{1-x}Sm_x)NbO_4$ (x = 0.02–0.15) ceramics

Keywords:
Ceramics
Crystal structure
Rietveld refinement
Bond ionicity
Lattice energy
Bond energy

A B S T R A C T

In this paper, the effects of Nd^{3+} ions substitution with Sm^{3+} ions on the microwave dielectric properties of $NdNbO_4$ ceramics were investigated. X-ray diffraction patterns showed a single system with a monoclinic fergusonite structure of $NdNbO_4$ in the range of x = 0.02–0.15. In addition, the Rietveld refinement was used to investigate the crystal structure of the $NdNbO_4$ ceramics. The bond ionicity, lattice energy and bond energy were calculated to evaluate the correlations between complex chemical bond theory and the microwave dielectric properties. A small level of Sm^{3+} substitution (x = 0.08) could improve the Q × f value of the $NdNbO_4$ ceramics. The increasing Q × f value could be due to the increase in lattice energy. The dielectric constant ε_r and τ_f values were depended upon bond ionicity and bond energy. An excellent microwave dielectric properties with ε_r = 19.56, Q × f = 66,200 GHz and τ_f = −28.37 ppm/°C was obtained when x = 0.08 in the $(Nd_{1-x}Sm_x)NbO_4$ system.

1. Introduction

The microwave dielectric ceramics plays an important role in the development of glob positioning systems, intelligent transport systems and satellite broadcasting [1,2]. Requirements for the microwave dielectric ceramics should have high relative permittivity ($\varepsilon_r > 10$) for miniaturization, high quality factor ($Q \times f > 10{,}000$ GHz) for better selectivity and near zero temperature coefficient of resonant frequency ($\tau_f = 0$ ppm/°C) for the system stability [3,4]. In order to meet the specifications of current and future development, numbers researchers are focusing on exploring new excellent microwave dielectric materials.

In recent years, the $NdNbO_4$ ceramics which are firstly reported by *Kim* et al., have attracted a great deal of interest due to its electrical and structural characterization [5,6]. Researches on the $NdNbO_4$ materials have been ongoing and reported for a long time. For example, *Zhang* et al. [7]. reported that the microwave dielectric properties of $NdNbO_4$ doping with 2.0 wt.% CaF_2 sintered at 1225 °C for 4 h shows excellent microwave dielectric properties with ε_r ~20.1, $Q \times f$ ~75, 000 GHz and τ_f ~ −19.16 ppm/°C. Doping with 0.6 wt.% $CaTiO_3$ obtained a high $Q \times f$ value for the $NdNbO_4$ ceramics sintered at 1275 °C for 4 h [8]. Then they discovered that the microwave properties of $NdNbO_4$ ceramics could be optimized using bivalent ions substituted to Nd^{3+}ionic owing to formation of solid solutions, and the phase composition changed as the Nd^{3+} ionic substituted by these bivalent ions (Sr^{2+}, Ca^{2+}, Mn^{2+}, Co^{2+}) [9,10]. The effects of Ta^{5+} and Sb^{5+} ions substitution for the $NdNbO_4$ ceramics are also investigated, a small level of Sb^{5+} substitution (x = 0.06) could greatly improve the Q × f values of the $NdNbO_4$ ceramics [11,12]. Moreover, phase change is also investigated and proved to play an important role in $NdNbO_4$ ceramics. However, few works are reported about the effects of trivalent ions substitution on the microwave dielectric properties of $NdNbO_4$ ceramics. In addition, the relationship between bond ionicity, lattice energy, bond energy and microwave dielectric properties of $(Nd_{1-x}Sm_x)NbO_4$ is also not discussed.

Therefore, in this paper, the correlations between crystal structure and microwave dielectric properties of $(Nd_{1-x}Sm_x)NbO_4$ were systematically discussed. The bond ionicity, lattice energy and bond energy were calculated based on the complex chemical bond theory. Moreover, an available method based on the Rietveld refinement of X-ray techniques was also used to analyze the structures of crystalline phases.

2. Experimental procedure

The $(Nd_{1-x}Sm_x)NbO_4$ (x = 0.02–0.15) ceramics were prepared via the solid–state reaction method, using high-purity (99.9%) Nd_2O_3, Sm_2O_3, and Nb_2O_5 powders. A stoichiometric mixture of the $(Nd_{1-x}Sm_x)NbO_4$ compounds was ball-milled with distilled water for 6 h. After calcinations at 900 °C for 4 h, the obtained powders were re-milled 6 h. Then, the dried powders with 6 wt% paraffin as a binder were granulated by sieving through an 80 mesh, and pressed into pellets with 10 mm diameter and 5 mm thickness at 100 MPa. Then these pellets were sintered at temperatures of 1225–1275 °C for 4 h in the air.

The crystal structures of the synthesized samples were identified by X-ray diffraction (XRD, Rigaku D/max 2550 PC, Tokyo, Japan)

http://dx.doi.org/10.1016/j.jallcom.2015.09.064
0925-8388/

with Cu Kα radiation generated at 40 kV and 40 mA. The XRD data were deal and analyzed using the Rietveld refinement method by the Full-Prof software. The microstructure of the ceramic surfaces were performed and analyzed by a scanning electron microscopy (SEM, MERLIN Compact, Germany). The microwave dielectric properties were measured in the frequency range of 8–13 GHz using a HP8720ES network analyzer. The temperature coefficients of resonant frequency (τ_f) were measured in the temperature range from 25 °C to 85 °C. The τ_f (ppm/°C) was calculated by noting the change in resonant frequency (Δf)

$$\tau_f = \frac{f_2 - f_1}{f_1(T_2 - T_1)} \quad (1)$$

where f_1 was resonant frequency at T_1 and f_2 was the resonant frequency at T_2.

The apparent densities of the sintered pellets were measured using the Archimedes method (Mettler ToledoXS64). To study the relative density of the sample, the theoretical density was obtained from the crystal structure and atomic weight by the Eq. (2) [13]:

$$\rho\text{theory} = \frac{ZA}{V_C N_A} \quad (2)$$

where V_C, N_A, Z, and A are volume of unit cell (cm^3), avogadro number (mol^{-1}), number of atoms in unit cell, and atomic weight (g/mol), respectively. The relative density was obtained by the Eq. (3):

$$\rho\ relative\ = \frac{\rho bulk}{\rho theory} \times 100\% \quad (3)$$

3. Results and discussion

The XRD patterns of $(Nd_{1-x}Sm_x)NbO_4$ (x = 0.02–0.15) composites over a range of x vales are shown in Fig. 1. All of the peaks are clearly indexed as the monoclinic phase for $NdNbO_4$ (ICSD #32-0680) in the range of x = 0.02 to 0.15, no additional phase is observed. In order to clarify the effects of Sm^{3+} ionic substitution for Nd^{3+} ionic on the crystal structure of $(Nd_{1-x}Sm_x)NbO_4$ ceramics, all parameters of interest including scale factors for all phases, zero point, background, half-width, asymmetry parameters, unit-cell parameters, atomic positional coordinates, temperature factors are refined step-by-step for avoiding correlations using Full-Prof software. The structural refinement patterns of the $(Nd_{0.92}Sm_{0.08})NbO_4$ ceramic are offered in Fig. 2, and the refined lattice parameters, cell volume, reliability factors, bond length, are presented in Table 1. As shown in Table 1, the lattice parameters

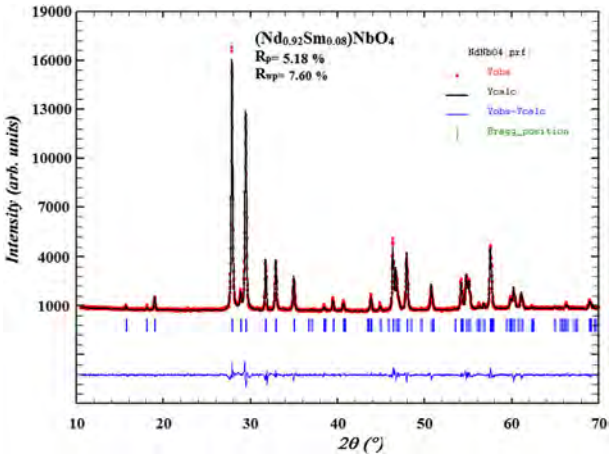

Fig. 2. The profile fits for the Rietveld refinement of $(Nd_{0.92}Sm_{0.08})NbO_4$ ceramic.

and cell volumes slightly decreased with increasing Sm^{3+} ionic contents, which is due to the incorporation of smaller Sm^{3+}(1.079 Å, CN = 8) in place of Nd^{3+}(1.109 Å, CN = 8) [14]. However, the lattice parameters generally increases with increase in Sm^{3+} ionic up to 0.08 mol, which could be due to the change in the crystal structure of the $NdNbO_4$ ceramics.

Fig. 3 shows the SEM images of the $(Nd_{1-x}Sm_x)NbO_4$ (x = 0.02–0.15) ceramics sintered 1250 °C for 4 h. As shown in Fig. 3 (a)–(d), it can be seen that all of the grains have no obvious change, and the grains of all the specimens are homogeneous and the surface is smooth. Moreover, all the estimated mean particle size is in the range of 3–5 μm. With a further increase of Sm^{3+} ions, decreased in grain size and some pores can be seen in Fig. 3(e)–(f), which shows evidence of porosity consistent with a lower bulk density. It suggests that exceed Sm^{3+} ions substitution have no benefits to the densification of the $(Nd_{1-x}Sm_x)NbO_4$ ceramics.

In general, the ε_r values have close relationship with the relative density, dielectric polarizabilities and structural characteristics such as the distortion, tilting and rattling spaces of oxygen octahedron in the unit cell [14–16]. In this study, the relative density is not under consideration in the ε_r values owing to the homogeneous SEM photos from the Fig. 3. Therefore, the ε_r values are dependent on the dielectric polarizabilities and structural characteristics. In our previous work, we reported the effects of bond ionicity on the ε_r values for the $NdNbO_4$ system [17]. Their relationship written as follows:

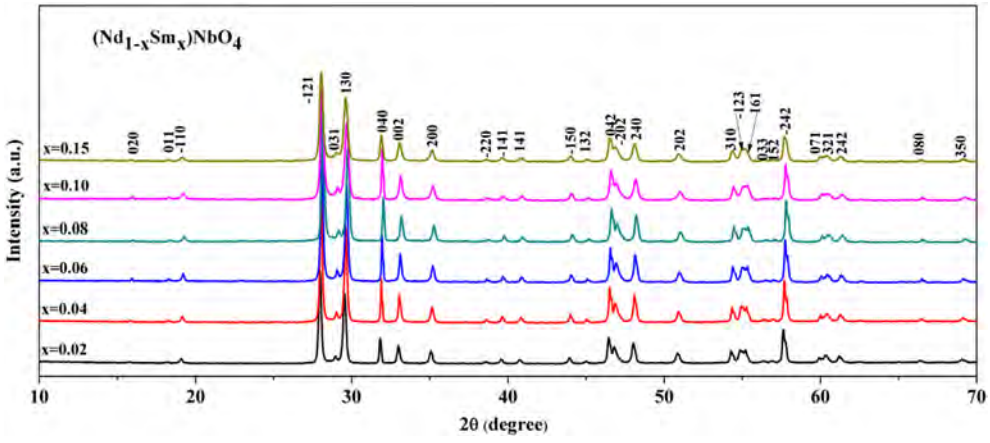

Fig. 1. The XRD patterns of $(Nd_{1-x}Sm_x)NbO_4$ ($0.02 \leq x \leq 0.15$) ceramics sintered at 1250 °C for 4 h.

Table 1
Crystallographic data from Rietveld refinement for $(Nd_{1-x}Sm_x)NbO_4$ $(0.02 \le x \le 0.15)$ ceramics sintered at 1250 °C for 4 h.

x value	*x = 0.02*	*x = 0.04*	*x = 0.06*	*x = 0.08*	*x = 0.10*	*x = 0.15*
a	5.4630	5.4599	5.4572	5.4537	5.4570	5.4594
b	11.2715	11.2756	11.2745	11.2663	11.2688	11.2745
c	5.1476	5.1461	5.1456	5.1433	5.1434	5.1455
β	94.445	94.446	94.420	94.426	94.450	94.453
$V_{cell}(Å^3)$	316.30	315.86	315.65	315.08	315.34	315.76
R_p	0.1360	0.1400	0.1270	0.0518	0.1220	0.1340
R_{wp}	0.1400	0.1510	0.1300	0.0760	0.1350	0.1490
$Nd/Sm–O(1)^1(Å)$	2.5774	2.5772	2.5769	2.5751	2.5954	2.5965
$Nd/Sm–O(1)^2(Å)$	2.4833	2.4826	2.4815	2.4802	2.4538	2.4549
$Nd/Sm–O(2)^1(Å)$	2.6149	2.6150	2.6144	2.6128	2.6419	2.6432
$Nd/Sm–O(2)^2(Å)$	2.4320	2.4310	2.4308	2.4292	2.3553	2.3563
$Nb–O(1)^1(Å)$	1.8920	1.8915	1.8907	1.8897	1.8685	1.8693
$Nb–O(1)^2(Å)$	2.3394	2.3392	2.3391	2.3376	2.3899	2.3910
Nb–O(2)(Å)	1.7020	1.7026	1.7025	1.7015	1.7636	1.7644

$$\varepsilon_r = \frac{n^2 - 1}{1 - f_i} + 1 \tag{4}$$

where n is the refractive index. It indicates that the dielectric constant decreased with the bond ionicity decreasing. The bond ionicity f_i calculated using the generalized P–V-L dielectric theory as follows [17]:

$$f_i^{\mu} = \frac{(C^{\mu})^2}{\left(E_g^{\mu}\right)^2} \tag{5}$$

$$f_C^{\mu} = \frac{\left(E_h^{\mu}\right)^2}{\left(E_g^{\mu}\right)^2} \tag{6}$$

where f_i^{μ} is the bond ionicity and f_c^{μ} is bond covalency E_g^{μ} is the average energy gap for the type bond μ, which is composed of homopolar E_h^{μ} and heteropolar C^{μ} parts as follows:

$$\left(E_g^{\mu}\right)^2 = \left(E_h^{\mu}\right)^2 + (C^{\mu})^2 \tag{7}$$

where

$$\left(E_h^{\mu}\right)^2 = \frac{39.74}{(d^{\mu})^{2.48}} \tag{8}$$

For any binary crystal A_mB_n type compounds, the heteropolar C^{μ} parts can be calculated as following:

$$C^{\mu} = 14.4 b^{\mu} \exp\left(-k_s^{\mu} r_o^{\mu}\right)\left[\left(\frac{\left(Z_A^{\mu}\right)^*}{r_o^{\mu}} - (n/m)\frac{\left(Z_B^{\mu}\right)^*}{r_o^{\mu}}\right)\right] (\text{ if } n > m) \tag{9}$$

$$C^{\mu} = 14.4 b^{\mu} \exp\left(-k_s^{\mu} r_o^{\mu}\right)\left[\left((m/n)\frac{\left(Z_A^{\mu}\right)^*}{r_o^{\mu}} - \frac{\left(Z_B^{\mu}\right)^*}{r_o^{\mu}}\right)\right] (\text{ if } n < m) \tag{10}$$

where b^{μ} is a correction factor that is proportional to the square of the average coordination number N_c^{μ}, $\left(Z_A^{\mu}\right)^*$ is the effective number of valence electrons on the cation A and $\left(Z_B^{\mu}\right)^*$ is the effective number of valence electrons on the anion B. Table 2 shows the calculated results of bond ionicity for $(Nd_{1-x}Sm_x)NbO_4$ $(0.02 \le x \le 0.15)$ ceramics. According to calculated results, Fig. 4 shows the ε_r values and the average of Nd-site bond ionicity Af_i of $(Nd_{1-x}Sm_x)NbO_4$ $(0.02 \le x \le 0.15)$ ceramics sintered at 1250 °C for 4 h. With the substitution ions increasing, the ε_r values keep the similar tendency with the Af_i, and then both of them decreased. This is due to high substitution ions would result in low bond ionicity, and low bond ionicity correlates with low polarizabilities, when the polarizabilities decreased, the ε_r values decreased.

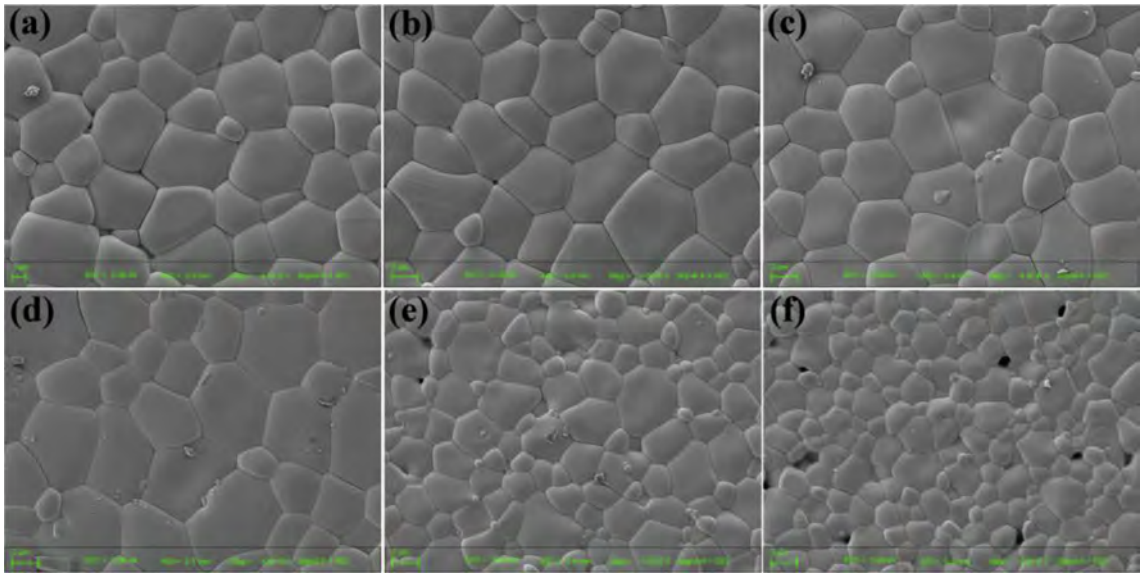

Fig. 3. The SEM photographs of $(Nd_{1-x}Sm_x)NbO_4$ $(0.02 \le x \le 0.15)$ ceramics sintered at1250 °C for 4 h.

As we all known, the Q × f values were affected by many factors, and it can be divided into two fields, the intrinsic loss and extrinsic loss. The intrinsic losses are mainly caused by lattice vibration modes, while the extrinsic losses are dominated by second phases, oxygen vacancies, grain boundaries, and densification or porosity [12,17,18]. In this work, the effect of extrinsic loss is minimal due to the densified compounds (>93%) and the homogeneous grains. Moreover, the grain sizes of the substituted $NdNbO_4$ have no significant difference, all in the range of 3–5 μm. And the extrinsic loss can only be a general discussion point as it is difficult to quantitatively relate changes in quality factor. Therefore, in the recent researches, we reported that the Q × f values with oxygen octahedron structure are observed to affect by the lattice energy [11–13]. With an increase in the lattice energy, the Q × f values would increase. Based on the generalized P–V-L theory [19], the ionic and covalent parts make contribution to the lattice energy for anyone single-bond crystal. The ionic part contribution to the crystal lattice energy mainly results from electrostatic interactions and repulsive interactions of the ion pairs, and another arises from the overlap of electron clouds. And the lattice energy U_{cal} of a complex crystal can be calculated as follows:

$$U_{cal} = \sum_{\mu} U_b^{\mu} \tag{11}$$

$$U_b^{\mu} = U_{bc}^{\mu} + U_{bi}^{\mu} \tag{12}$$

$$U_{bc}^{\mu} = 2100m\frac{(Z_+^{\mu})^{1.64}}{(d^{\mu})^{0.75}}f_C^{\mu} \tag{13}$$

$$U_{bi}^{\mu} = 1270\frac{(m+n)Z_+^{\mu}Z_-^{\mu}}{d^{\mu}}\left(1-\frac{0.4}{d^{\mu}}\right)f_i^{\mu} \tag{14}$$

where U_{bc}^{μ} is the covalent part and U_{bi}^{μ} is the ionic part of μ bond. Z_+^{μ} and Z_-^{μ} are the valence states of cation and anion which constituted to the bond μ. f_i and f_c are the bond ionicity and bond covalency. The calculated lattice energy for $(Nd_{1-x}Sm_x)NbO_4$ (x = 0.02–0.15) is illustrated in Table 3. Based on the calculated results, the relationship between Q × f values and lattice energy is given in Fig. 5. With the Sm^{3+} ions substitution contents increasing, the lattice energy increased resulted in the increased Q × f value in the range of x = 0.02–0.08. When x > 0.08, the lattice energy decreased, the Q × f values decreased.

Our recent work [12,18] indicates that the bond energy can affect the temperature coefficient of resonant frequency τ_f values, and higher bond energy correlates a smaller $|\tau_f|$ value. The bond energy E of a complex crystal could be written as:

$$E = \sum_{\mu} E_b^{\mu} \tag{15}$$

where E_b^{μ} is bond energy for the type μ bond, which is composed of nonpolar covalence energy E_c^{μ} and complete ionicity energy E_i^{μ} parts as follows:

$$E_b^{\mu} = t_c E_c^{\mu} + t_i E_i^{\mu} \tag{16}$$

The energy of the ionic form E_i^{μ} was the unit charge product divided by the bond length d^{μ}, adjusted to kcal/mol by the factor

Table 2
Bond ionicity for $(Nd_{1-x}Sm_x)NbO_4$ (0.02 ≤ x ≤ 0.15) ceramics.

Bond type	Bond ionicity f_i (%)					
	x = 0.02	x = 0.04	x = 0.06	x = 0.08	x = 0.10	x = 0.15
Nd/Sm–O(1)[1]	90.3161	90.3082	90.3074	90.3060	90.2898	90.2906
Nd/Sm–O(1)[2]	90.2176	90.2091	90.2073	90.2062	90.1401	90.1413
Nd/Sm–O(2)[1]	80.7527	80.7390	80.7372	80.7354	80.7158	80.7174
Nd/Sm–O(2)[2]	80.4060	80.3902	80.3888	80.3858	80.1423	80.1447
Nb–O(1)[1]	88.4124	88.4027	88.4006	88.3922	88.3197	88.3211
Nb–O(1)[2]	88.8176	88.8080	88.8073	88.8075	88.7692	88.7690
Nb–O(2)	77.9071	77.8958	77.8944	77.8903	78.1004	78.1035
A $f_{i\ (Nd/Sm-O)}$[a]	85.2614	85.2504	85.2490	85.2472	85.2110	85.2125

[a] The A $f_{i(Nd/Sm-O)}$ was the average of the bond ionicity of bond Nd/Sm–O.

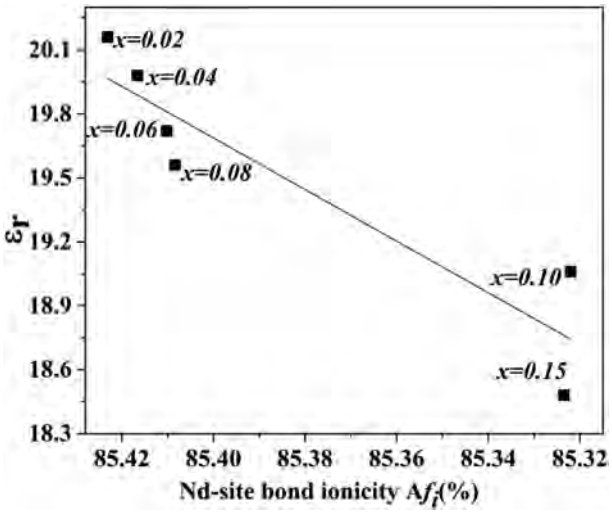

Fig. 4. The ε_r values and the average of Nd-site bond ionicity Af_i of $(Nd_{1-x}Sm_x)NbO_4$ (0.02 ≤ x ≤ 0.15) ceramics sintered at 1250 °C for 4 h.

Table 3
Lattice energy for $(Nd_{1-x}Sm_x)NbO_4$ (0.02 ≤ x ≤ 0.15) ceramics.

Bond type	Lattice energy U (kJ/mol)					
	x = 0.02	x = 0.04	x = 0.06	x = 0.08	x = 0.10	x = 0.15
Nd/Sm–O(1)[1]	1420	1421	1421	1422	1412	1412
Nd/Sm–O(1)[2]	1463	1465	1465	1466	1478	1477
Nd/Sm–O(2)[1]	1326	1326	1326	1326	1315	1314
Nd/Sm–O(2)[2]	1405	1406	1407	1407	1442	1442
Nb–O(1)[1]	7204	7206	7207	7211	7270	7267
Nb–O(1)[2]	6132	6132	6132	6134	6028	6026
Nb–O(2)	7013	7011	7011	7014	6839	6836
Total U	25,963	25,967	25,969	25,980	25,784	25,774

The energy of the ionic form E_i^{μ} was the unit charge product divided by the bond length d^{μ}, adjusted to kcal/mol by the factor

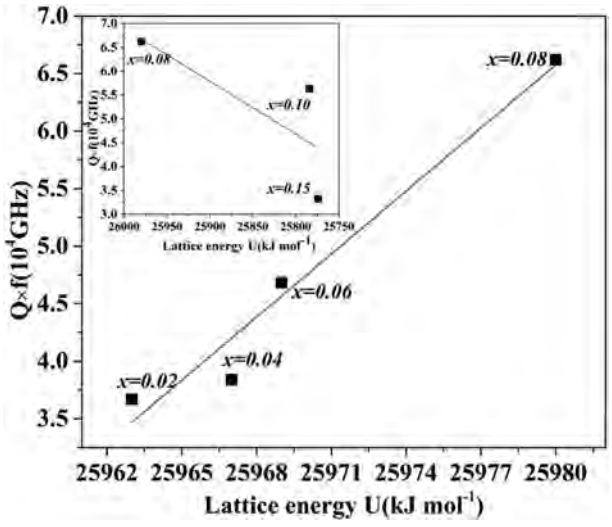

Fig. 5. The Q × f values of $(Nd_{1-x}Sm_x)NbO_4$ (0.02 ≤ x ≤ 0.15) ceramics as a function of lattice energy.

33200 when the bond length is pm.

$$E_i^{\mu} = \frac{33200}{d^{\mu}} \tag{17}$$

For any binary crystal A_mB_n type compounds, the nonpolar covalence energy E_c^{μ} parts could be calculated as following:

$$E_c^{\mu} = \frac{(r_{cA} + r_{cB})}{d^{\mu}}(E_{A-A}E_{B-B})^{1/2} \tag{18}$$

where r_{cA} and r_{cB} are the covalent radii, E_{A-A} and E_{B-B} were the homonuclear bond energy, which can be obtained from the handbook of bond energies [20].

For the Eq. (16), t_c and t_i are the covalent and ionic blending coefficients, respectively. The relationship of t_c and t_i can be described by the following formula:

$$t_c + t_i = 1 \tag{19}$$

The ionic blending coefficient t_i is defined as:

$$t_i = \left|\frac{(S_A - S_B)/\Delta S_B}{2}\right| \tag{20}$$

where S_A and S_B are the electronegativities of A and B ions, in this paper, $S_{Nd} = 1.14$, $S_{Sm} = 1.17$, $S_{Nb} = 1.6$ and $S_O = 3.44$. ΔS_B is the change for complete of an electron and has the value of 3. The details of bond energy are given in Table 4. Fig. 6 shows the τ_f values of $(Nd_{1-x}Sm_x)NbO_4$ ceramics as a function of bond energy. As Fig. 6 shows, the variation of τ_f values is consistent with the bond energy. With the decrease of the bond energy, the $|\tau_f|$ values decreased. Therefore, lower bond energy correlates with bigger $|\tau_f|$ value, bigger $|\tau_f|$ value indicates the system would be more instable.

The relative densities, the ε_r values, the $Q \times f$ values and the τ_f values of $(Nd_{1-x}Sm_x)NbO_4$ ($x = 0.02–0.15$) are given in Table 5. Moreover, excellent microwave dielectric properties of $(Nd_{0.92}Sm_{0.08})NbO_4$ ceramics with $\varepsilon_r = 19.56$, $Q \times f = 66{,}200$ GHz and $\tau_f = -28.37$ ppm/°C are obtained at 1250 °C for 4 h.

4. Conclusions

The correlations between bond ionicity, lattice energy, bond energy and the microwave dielectric properties of $(Nd_{1-x}Sm_x)NbO_4$ ($x = 0.02–0.15$) ceramics were investigated carefully in this study. The Rietveld refinement reveals that $NdNbO_4$ ceramics perform the monoclinic fergusonite structure with the space group I2/a (no. 15). With a decrease in bond ionicity, the ε_r values decreased, which is due to the low dielectric polarizabilities. Higher $Q \times f$ values correlate with higher lattice energy. The τ_f values of the specimens are really dependent on the bond energy. As the bond energy decreased, the τ_f values shift to the negative direction, indicates that the system tend to instable. Moreover, at 1250 °C, the $(Nd_{1-x}Sm_x)NbO_4$ ceramics with $x = 0.08$ possesses excellent microwave dielectric properties with an ε_r value of 19.56, $Q \times f$ value of 66,200 GHz and τ_f value of −28.37 ppm/°C.

Table 4
The bond energy for $(Nd_{1-x}Sm_x)NbO_4$ ($0.02 \le x \le 0.15$) ceramics.

Bond type	Bond energy E (kJ/mol)					
	x = 0.02	x = 0.04	x = 0.06	x = 0.08	x = 0.10	x = 0.15
Nd/Sm–O(1)^1	321.41	320.96	320.52	320.27	317.29	315.29
Nd/Sm–O(1)^2	333.59	333.19	332.85	333.52	335.60	334.18
Nd/Sm–O(2)^1	316.80	316.32	315.93	315.65	311.70	310.37
Nd/Sm–O(2)^2	340.63	340.27	339.79	339.50	349.63	348.17
Nb–O(1)^1	614.44	614.40	614.86	615.19	622.17	621.90
Nb–O(1)^2	496.93	496.97	496.99	497.31	486.43	486.21
Nb–O(2)	683.03	682.97	682.83	683.23	659.17	658.88
Total E	3106.83	3105.10	3103.77	3103.67	3081.99	3075.67

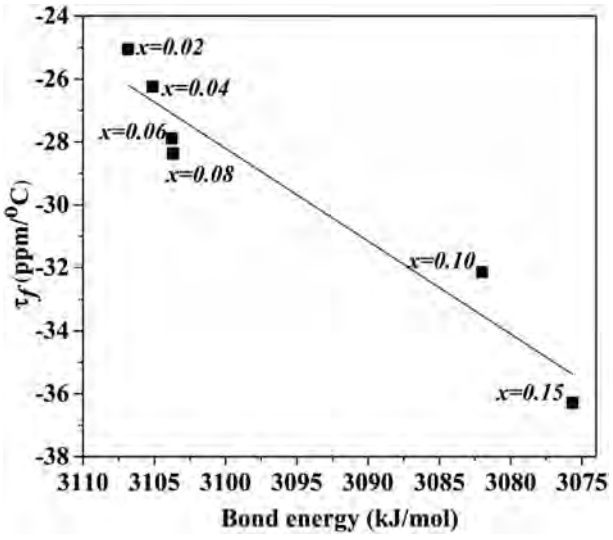

Fig. 6. The bond energy (kJ mol^{-1}) and τ_f values of $(Nd_{1-x}Sm_x)NbO_4$ ($0.02 \le x \le 0.15$) ceramics sintered at 1250 °C for 4 h.

Table 5
The relative density and the microwave dielectric properties of $(Nd_{1-x}Sm_x)NbO_4$ ($0.02 \le x \le 0.15$) ceramics sintered at 1250 °C for 4 h.

x value	Relative density	ε_r	Q × f (GHz)	τ_f (ppm/°C)
0.02	95.48%	20.16	36,700	−25.06
0.04	95.59%	19.98	38,400	−26.24
0.06	95.27%	19.72	46,800	−27.89
0.08	95.99%	19.56	66,200	−28.37
0.10	93.36%	19.16	56,300	−32.14
0.15	93.02%	18.98	33,200	−36.29

Acknowledgments

The authors gratefully acknowledged supports from the Key Laboratory of Advanced Ceramics and Machining Technology, Ministry of Education (Tianjin University).

References

[1] M. Makimoto, S. Yamashita, Springer. Berlin. 2001.
[2] S. Nomura, Ferroelectrics 49 (1983) 61–70.
[3] Y.B. Chen, J. Alloy. Compd. 478 (2009) 781–784.
[4] L. Nedelcu, M.I. Toacsan, M.G. Banciu, A. Ioachim, J. Alloy. Compd. 509 (2011) 477–481.
[5] D.W. Kim, D.K. Kwon, S.H. Yoon, K.S. Hong, J. Am. Ceram. Soc. 89 (2006) 3861–3864.
[6] K.P.F. Siqueira, R.L. Moreira, A. Dias, Chem. Mater 22 (2010) 2668–2674.
[7] P. Zhang, T. Wang, W.S. Xia, L.X. Li, J. Alloy. Compd. 535 (2012) 1–4.
[8] P. Zhang, Z.K. Song, Y. Wang, et al., J. Alloy. Compd. 581 (2013) 741–746.
[9] P. Zhang, Z.K. Song, Y. Wang, L.X. Li, J. Am. Ceram. Soc. 97 (2014) 976–981.
[10] Z.K. Song, P. Zhang, Y. Wang, L.X. Li, J. Alloy. Compd. 583 (2014) 546–549.
[11] P. Zhang, Y.G. Zhao, et al., J. Alloy. Compd. 640 (2015) 90–94.
[12] P. Zhang, Y.G. Zhao, X.Y. Wang, J. Alloy. Compd. 644 (2015) 621–625.
[13] I.D. Brown, R.D. Shannon, Acta. Cryst. 29 (1973) 266–282.
[14] R.D. Shannon, Acta. Crystallogr. A32 (1976) 751–767.
[15] C.L. Huang, J.Y. Chen, J. Am. Ceram. Soc. 93 (2010) 1248–1251.
[16] W.S. Kim, K.H. Yoon, E.S. Kim, J. Am. Ceram. Soc. 83 (2008) 2327–23279.
[17] P. Zhang, Y.G. Zhao, Y.X. Wang, Dalton. Trans. 44 (2015) 10932–10938.
[18] P. Zhang, Y.G. Zhao, X.Y. Wang, J. Alloy. Compd. 647 (2015) 386–391.
[19] D.T. Liu, S.Y. Zhang, Z.J. Wu, Inorg. Chem. 42 (2003) 2465–2469.
[20] Y.R. Luo, Comprehensive Handbook of Chemical Bond Energies, CRC Press, 2007.

Ping Zhang*, Yonggui Zhao
School of Electronic and Information Engineering, Key Laboratory of Advanced Ceramics and Machining Technology of Ministry of Education, Tianjin University, Tianjin 300072, PR China

* Corresponding author.
E-mail address: zptai@163.com (P. Zhang).

15 August 2015
Available online 10 September 2015